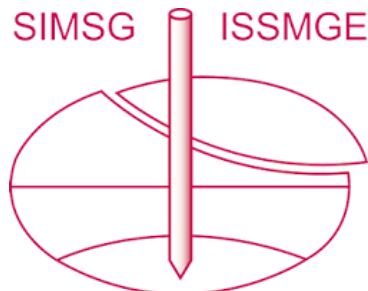


# INTERNATIONAL SOCIETY FOR SOIL MECHANICS AND GEOTECHNICAL ENGINEERING



*This paper was downloaded from the Online Library of the International Society for Soil Mechanics and Geotechnical Engineering (ISSMGE). The library is available here:*

*<https://www.issmge.org/publications/online-library>*

*This is an open-access database that archives thousands of papers published under the Auspices of the ISSMGE and maintained by the Innovation and Development Committee of ISSMGE.*

# Distribution of Stress Beneath a Rigid Foundation

## Distribution réelle des contraintes sous une fondation rigide

by Edgar SCHULTZE, Professor Dr.-Ing, Technische Hochschule Aachen, Germany

### Summary

The distribution of contact pressure for an axially loaded rigid foundation for the elastic isotropic half space can be calculated by the Boussinesq method. Using this method, the stresses at the edges become infinite, but this does not occur in practice because of plastic flow. Stress calculated according to Boussinesq is combined with plastic flow along the edges, which can be calculated by the equations for shear failure under foundations derived by Prandtl and Buisman, an improved distribution of pressure is obtained. For this elastic-plastic state, the equation for the contact pressure distribution is derived. The pressure distribution thus obtained varies with the factor of safety against shear failure under the structure and may have in the limiting case (factor of safety equal to 1) a full parabolic form. According to the theory, for the usual factors of safety which lie roughly between 2 and 3, the concave parabolic form is predominant.

Measurements of the distribution of contact pressure under structures are carried out for rigid foundations such as piers, for which measuring conditions are particularly favourable. Eleven case records from Germany and other countries are available, where the contact pressure distribution has been measured by several load gauges, particularly under piers, but also under columns, weirs and other structures on strata of gravel, sand, silt and boulder clay. The results of these measurements are presented in uniform cross-sections and plans in order to be able to make a comparison with the theoretical considerations. Eight cases show a concave parabolic distribution.

A completely parabolic distribution of stress was found for only three structures on cohesive soils. It is thus reasonable to conclude that the assumptions on which determination of pressure distribution are based, agree closely with practical experience.

### Sommaire

Pour des fondations rigides, supportant une charge centrale, la distribution des pressions sous la semelle peut se calculer, comme on le sait, d'après Boussinesq, si l'on prend comme base un état élastique. Des pressions infiniment grandes apparaissent alors au bord, lesquelles ne peuvent se produire par suite de phénomènes plastiques. Si l'on combine l'état de contrainte selon Boussinesq avec un état plastique dans les zones marginales, qui peut être calculé d'après les équations de rupture du sol de Prandtl et Buisman, il en résulte une distribution des pressions sous la semelle qui se rapproche le plus de la réalité. L'équation de la distribution des pressions sur la semelle se déduit pour cet état plastico-élastique. La pression sur le sol alors obtenue varie avec le coefficient de sécurité à la rupture du sol sous l'ouvrage et, dans le cas limite (sécurité, à la rupture du sol = 1) cette pression peut prendre une forme parabolique convexe. Cependant, en ce qui concerne les sécurités à la rupture du sol, habituellement trouvées, et qui sont comprises entre deux et trois, c'est la forme parabolique concave qui prédomine d'après la théorie.

La plupart des mesures de distribution des pressions sur la semelle sous des ouvrages proviennent de piliers rigides, là, où les conditions de mesure sont particulièrement favorables. D'Allemagne et de l'étranger on a pu recueillir 11 cas pour lesquels, grâce à un nombre suffisant d'appareils de mesure la distribution des pressions sur la semelle a été mesurée, principalement sous des piles de ponts, mais également sous des poteaux, des ouvrages de soutènement, des barrages et d'autres ouvrages construits sur du gravier, du sable, du limon et des marnes à blocs. Les résultats de ces mesures sont tous représentés par des schémas en coupe et en plan afin de pouvoir faire une comparaison avec les considérations théoriques. Il se trouve que dans 8 cas on a affaire à une distribution parabolique concave. 3 ouvrages seulement, construits sur des sols cohérents, généralement d'âge assez ancien, présentent une distribution parabolique convexe. C'est pourquoi on est amené à conclure que les hypothèses qui ont servi de base au calcul de la distribution des pressions sur la semelle pour l'état plastico-élastique, correspondent bien à la réalité.

### 1. Theory.

1.1. *Elastic state : Concave parabolic distribution*—By adopting the Boussinesq method, the following equation for distribution of contact pressure for any axial loading on a rigid foundation has been developed :

$$p_s(x) = \frac{p}{\pi a} \cdot \frac{1}{\sqrt{1 - (x/a)^2}} \quad (1)$$

where  $a = B/2$ .

The distribution is independent of the modulus of compressibility  $E$  and is valid for the surface loading. The influence of the depth of foundation on the distribution is not examined,

but is comparatively small. In other respects the theoretical picture disturbs because the stresses at the edge of the foundation are infinite : no subsoil can successfully withstand such stresses. The elastic state is therefore obviously useless without modifications, even for small loads, and a different distribution of pressure will therefore apply.

1.2. *Plastic state : Full parabolic distribution*—If the load on the rigid strip is steadily increased, it reaches a maximum value at which the soil fails. The ultimate bearing resistance provides a contact pressure distribution which

consists of rectangles and triangles. The equation reads (Fig. 1) :

$$P_s(x) = cN_c + \gamma_1 N_q D + 4a \cdot \gamma_2 N_Y \left( 1 - \frac{x}{a} \right) \quad \dots \quad (2)$$

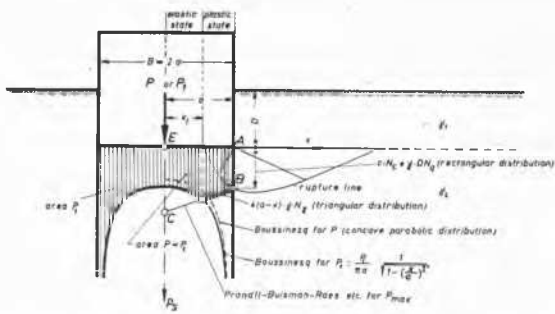


Fig. 1 Change in contact pressure distribution under a stiff foundation strip according to Boussinesq, with the emergence of plastic zones at the edge.

Modification de la répartition des pressions sous une fondation rigide d'après Boussinesq du fait des phénomènes plastiques marginaux.

= part of the apparent cohesion  $c$  of the soil (rectangular)  
+ part of the foundation depth  $D$  (rectangular) + part of the width  $B = 2a$  of the strip (triangular/roof-shaped).

The factors  $N$  depend upon the angle of internal friction of the soil, the assumed friction between foundation and subsoil, and the shape of the sliding planes which is most likely to indicate failure.

The contact pressure distribution now gives finite edge stresses which are compatible with the strength of the subsoil, but which in other respects are of exactly the opposite form to those under which the elastic state applies. Such pressure distribution is valid only for the ultimate failure load, so it is not always practicable and therefore does not provide a solution for the general case of a load of any value less than the failure value, as usually occurs in foundations.

**1.3. Elastic-plastic state : Mixed distribution**—Obviously we approach closer to reality by combining the elastic state according to Boussinesq with the plastic state according to Prandtl.

We start with the assumption that in the middle regions under the stiff strip, Boussinesq's distribution is valid, but that at the edge the bearing capacity can never be exceeded (Fig. 1).

As the area of the pressure diagram must remain constant for a given foundation load, the pressure is displaced towards the centre. The distance  $x_1$  from the centre line gives the point of transition from the elastic to the plastic state. There the stresses of Boussinesq (Equation 1) and those of Prandtl-Buisman (Equation 2) must be the same. By means of Boussinesq's distribution a part of the load  $P_1 > P$  is supported at the center of the strip.

By equating the stresses at the point of transition, we get :

$$\frac{P_1}{\pi a} \cdot \frac{1}{\sqrt{1-(x_1/a)^2}} = cN_c + \gamma_1 DN_q + 4a \cdot \gamma_2 N_Y \left( 1 - \frac{x_1}{a} \right) \quad (3)$$

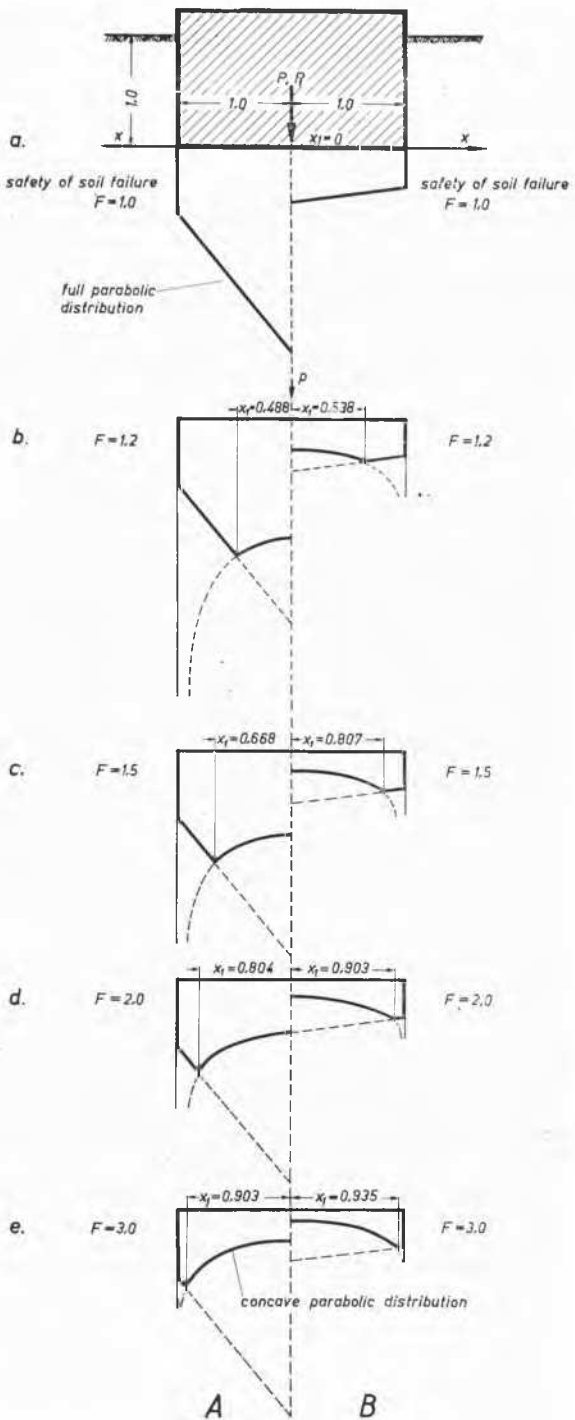


Fig. 2 Contact pressure distribution under a stiff foundation strip taking into account the plastic zone at the edge for varying factors of safety  $F$  and  $D/B = 0.5$ ;  $\gamma = 1.6 \text{ t/m}^3$ .

- (a) non cohesive soil :  $\phi = 30^\circ$ ;  $c = 0$ .
- (b) cohesive soil :  $\phi = 15^\circ$ ;  $c = 1 \text{ t/m}^2$ .

Distribution des pressions sous une fondation rigide compte tenu des phénomènes plastiques marginaux pour des coefficients de sécurité divers :  $F$  et  $D/B = 0.5$ ;  $\gamma = 1.6 \text{ t/m}^3$ .

- (a) sol non cohérent :  $\phi = 30^\circ$ ;  $c = 0$ ;
- (b) sol cohérent :  $\phi = 15^\circ$ ;  $c = 1 \text{ t/m}^2$ .

Moreover, the area of the shaded surface to the right of the centre line of Fig. 1 must be equal to  $P/2$

$$\frac{P}{2} = \frac{P_1}{\pi a} \int_0^{x_1} \frac{dx}{\sqrt{1 - (x/a)^2}} + a(cN_c + \gamma_1 DN_a) (1 - x_1/a) + 2a^2 \gamma_2 N_Y (1 - x_1/a)^2 \quad (4)$$

There are thus two equations for the two unknown quantities  $P_1$  and  $x_1$ . The solution to the integral in equation (4) is  $a \arcsin \frac{x_1}{a}$ .

According to Professor Dr.-Ing. Lohman (T.H. Aachen) the given quantities are best summarised as two constants :

$$C_1 = a(cN_c + \gamma_1 DN_a) \quad (5)$$

$$C_2 = 2a^2 \gamma_2 N_Y \quad (6)$$

Moreover we can write :

$$\xi = x/a \text{ and } \xi_1 = x_1/a \quad (7)$$

We then get :

$$\frac{P_1}{\pi} = \sqrt{1 - \xi_1^2} \cdot [C_1 + 2C_2(1 - \xi_1)] \quad (8)$$

$$\frac{P}{2} = \frac{P_1}{\pi} \cdot \arcsin \xi_1 + C_1(1 - \xi_1) + C_2(1 - \xi_1)^2 \quad (9)$$

Substituting from equation 8 in equation 9 we get :

$$\begin{aligned} \frac{P}{2} &= C_1 [\sqrt{1 - \xi_1^2} \cdot \arcsin \xi_1 + (1 - \xi_1)] + \\ &C_2 [2 \cdot \sqrt{1 - \xi_1^2} \cdot \arcsin \xi_1 \cdot (1 - \xi_1) + (1 - \xi_1)^2] \quad \dots \quad (10) \end{aligned}$$

$$\frac{P}{2} = C_1 \cdot f_{C_1}(\xi_1) + C_2 \cdot f_{C_2}(\xi_1) \quad (11)$$

The values of the two functions of  $\xi_1$  can be read from the table which has been prepared for this purpose.

Table

Numerical values  $f_{C_1}(\xi_1)$  and  $f_{C_2}(\xi_1)$  as a function of  $(\xi_1)$

$$f_{C_1}(\xi_1) = \sqrt{1 - \xi_1^2} \cdot \arcsin \xi_1 + (1 - \xi_1)$$

$$f_{C_2}(\xi_1) = 2 \cdot \sqrt{1 - \xi_1^2} \cdot \arcsin \xi_1 (1 - \xi_1) + (1 - \xi_1)^2$$

$\xi_1$	$f_{C_1}(\xi_1)$	$f_{C_2}(\xi_1)$
0,0	1,00000	1,00000
0,1	0,99966	0,98939
0,2	0,99727	0,95563
0,3	0,99068	0,89695
0,4	0,97716	0,81259
0,5	0,95345	0,70345
0,6	0,91479	0,57183
0,7	0,85375	0,42225
0,8	0,75638	0,26255
0,9	0,58810	0,10762
1,0	0,00000	0,00000

Equation (11) can be solved by trial and error by substituting various values of  $\xi_1$ . The quantity  $P_1$  is then determined using equation (8).

Distribution of contact pressure obtained in this way has been calculated as an example of a non-cohesive soil and of a cohesive soil for various factors of safety  $F$  of the ultimate resistance (Fig. 2). "Normal distribution" can be regarded as that acting with a factor of safety between 2 and 3 on ultimate bearing capacity.

These two values do not differ significantly from each other and, both for sand and for clay, mainly show a concave parabola with a slight lateral decline in stress at the edges with the depths of foundations normally used.

## 2. Pressure measurements beneath buildings.

The proof of a contact pressure distribution, as shown in Fig. 2d and 2e, is provided by the results of contact pressure measurements under completed buildings, where a certain depth of foundation is always present. Unfortunately, only few such measurements have been published. All available records were collected and set out schematically (Figs. 3-13). Further material is urgently needed, particularly in this field, in order to check the correctness of the theoretical considerations.

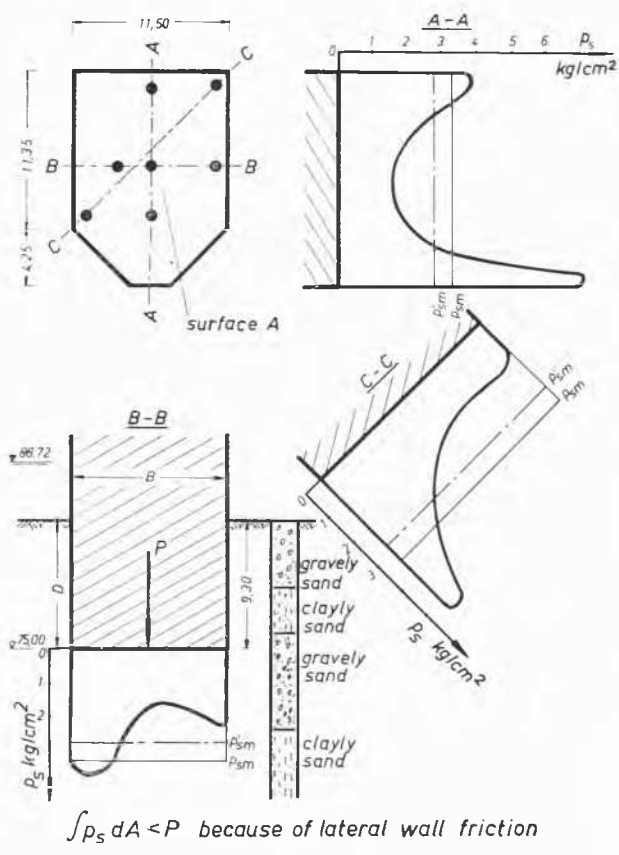


Fig. 3 Contact pressure distribution measured under a caisson of the Rhine bridge in Ludwigshafen 1932.  $D/B = 1.0$ . Distribution des pressions mesurées sous une pile du pont sur le Rhin à Ludwigshafen fondée par caisson pneumatique en 1932.  $D/B = 1.0$ . After : BURGER (1932). Der Bau der neuen Rheinbrücke bei Ludwigshafen (Rhein) - Mannheim. Baut. 10, p. 595.

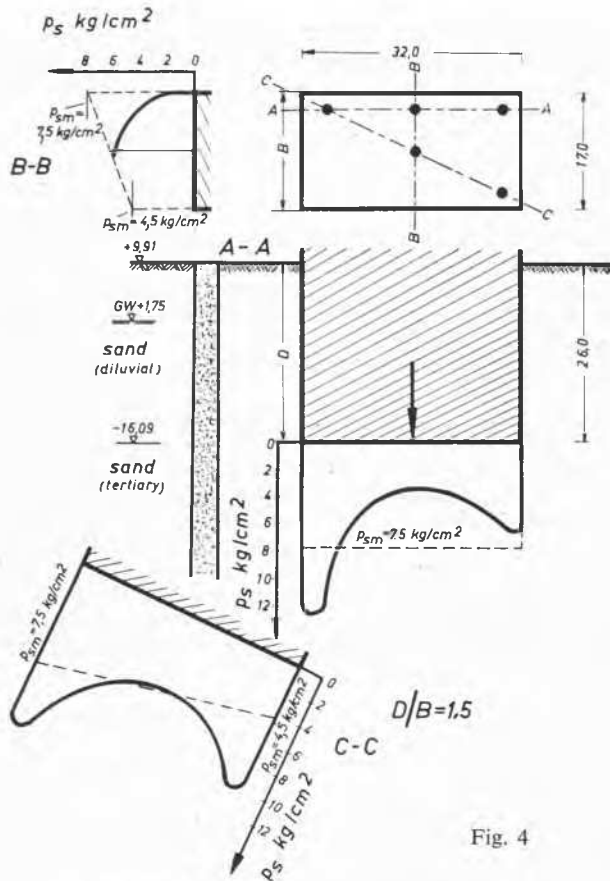


Fig. 4

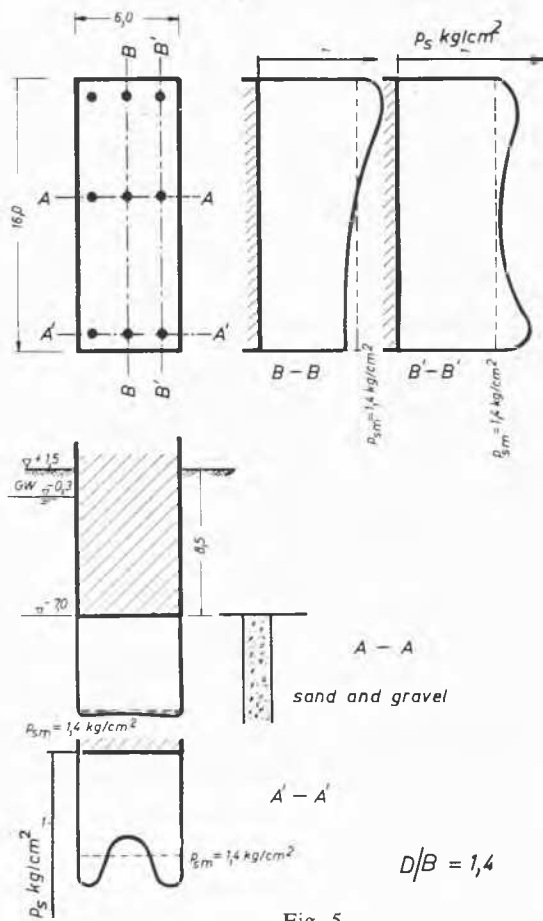


Fig. 5

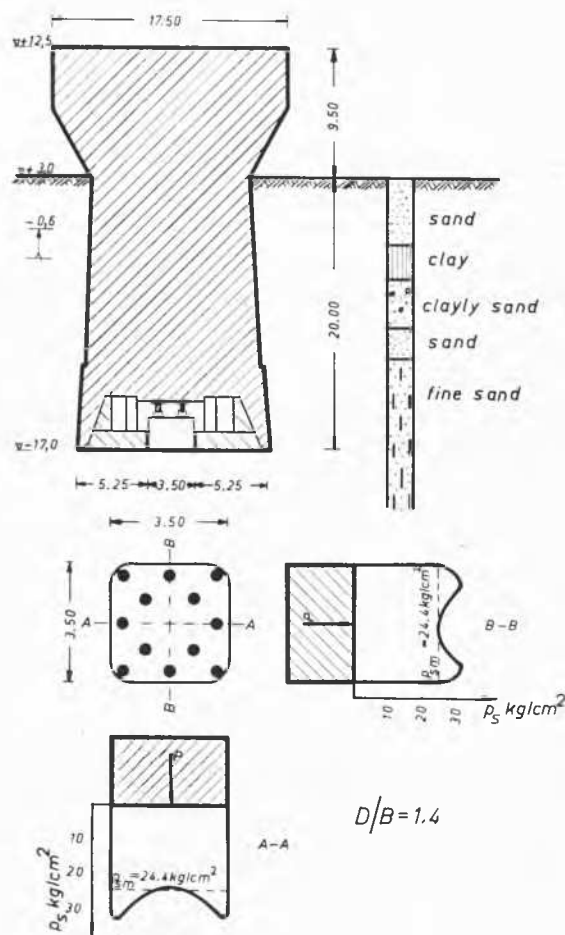


Fig. 6

Fig. 4 Contact pressure distribution measured under the east caisson of the Niederfinow ship-lift 1934.  $D/B = 1.5$   
Distribution des pressions mesurées sous le caisson d'est du monte-chARGE des bateaux Niederfinow 1934.  
 $D/B = 1.5$ .

After : DETIG (1934). Die Zwischenpfeiler der Kanalbrücke des Schiffshebewerks Niederfinow, Baut. 12, p. 522.

Fig. 5 Contact pressure distribution measured under a river pier of the Süderelbebrücke Hamburg-Harburg 1936.  $D/B = 1.4$ .  
Distribution des pressions mesurées sous une pile de pont sur le bras Sud de l'Elbe à Hamburg-Harburg 1936.  $D/B = 1.4$ .

After : Prospectus Fa. MAIHAK, Hamburg.

Fig. 6 Contact pressure distribution measured under the test caisson for highway suspension bridge near Hamburg 1938.  $D/B = 1.4$ .  
Distribution des pressions mesurées sous le caisson d'essai pour un pont suspendu de l'autostrade à Hamburg-Harburg 1936.  $D/B = 1.4$ .

After : SIEDEK (1948). Belastungsversuch in einem Senkkasten. Abh. Bodenmechanik und Grundbau, p. 88. Bielefeld.

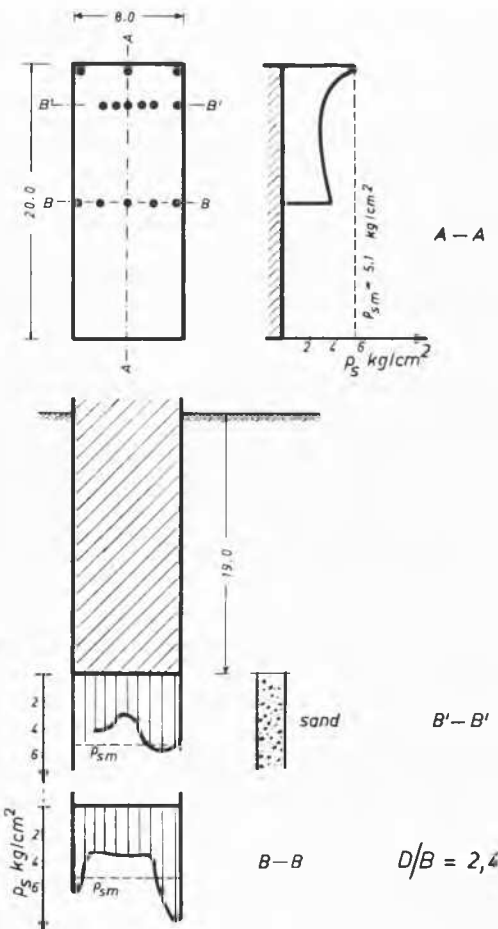


Fig. 7

Fig. 7. Contact pressure distribution measured under a caisson of the railway bridge in Kehl 1956.  $D/B = 2.4$ .

Distribution des pressions mesurées sous une pile fondée avec caisson pneumatique du pont de chemin de fer à Kehl 1956.  $D/B = 2.4$ .

After : Bundesanstalt für Wasserbau, Karlsruhe.

Fig. 8 Contact pressure distribution measured under the mushroom building in Berlin 1941.  $D/B = 1.6$ .

Distribution des pressions mesurées sous une construction en champignon à Berlin (1941).  $D/B = 1.6$ .

After : MUHS (1948). Durchführung und Ergebnis einer grossen Probobelastung Abh. Bodenmech. u. Grundb., p. 97, Bielefeld.

EBERT (1948). Messung der Druckverteilung im Baugrund mit Druckkissen, *ibidem*, p. 114.

Fig. 9 Contact pressure distribution measured under a square footing of the extension to the University of Glasgow, 1957.

Distribution des pressions mesurées sous une fondation superficielle de l'édifice élargi de l'université Glasgow, 1957.

After SUTHERLAND (1957). Diskussion IVth I.C.S.M.F.E. London, vol. III, p. 167.

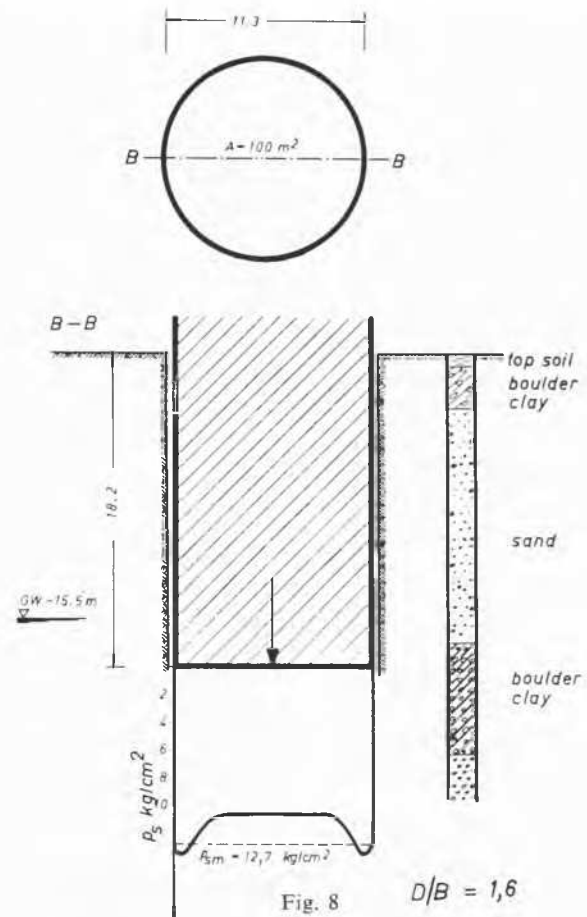


Fig. 8

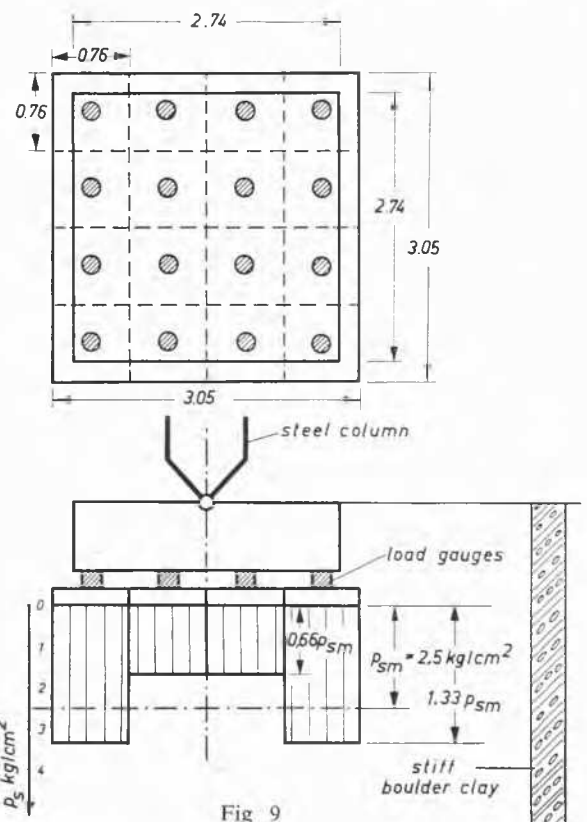


Fig. 9

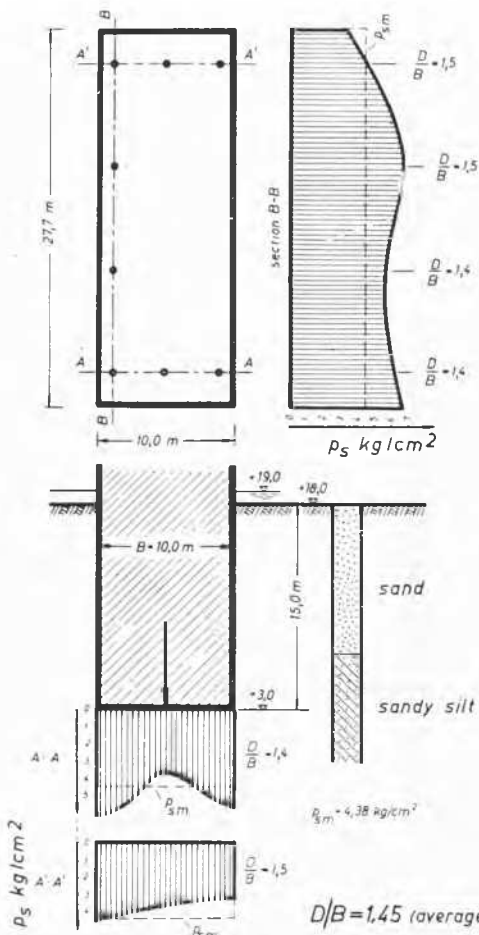


Fig. 10

Fig. 10 Contact pressure distribution measured under a pier of the Ponte Annibale Power plant on Volturno River (Italy) (1955).  $D/B = 1.45$  (averaged).

Distribution des pressions mesurées sur semelle du pilier de barrage à Volturno (en Italie) (1955).  $D/B = 1.45$  (en moyenne).

After : JAPELLI (1958). Pressioni sul piano di posa e cedimenti di un cassone penumatico, *Geotecnica*, 5, No. 4.

Fig. 11 Contact pressure distribution measured under a support foundation in the United States 1933.  $D/B = 1.6$ .

Distribution des pressions mesurées sous une fondation de soutien aux États-Unis. 1933.  $D/B = 1.6$ .

After : CONVERSE (1933). Distribution of pressure under a footing. Preliminary test of reactions under a square concret block reveal non uniform distribution of load. *Civ. Eng.* 3., p. 207.

Fig. 12 Contact pressure distribution measured under a support foundation in Texas 1933.

Distribution des pressions sous une fondation de soutien en Texas 1933.

After : GIESECKE-BADGET-EDDY (1933). The distribution of Soil pressure Beneath a footing. (*Bull Agricultural and Mechanical College of Texas* 4, Bull. 32).

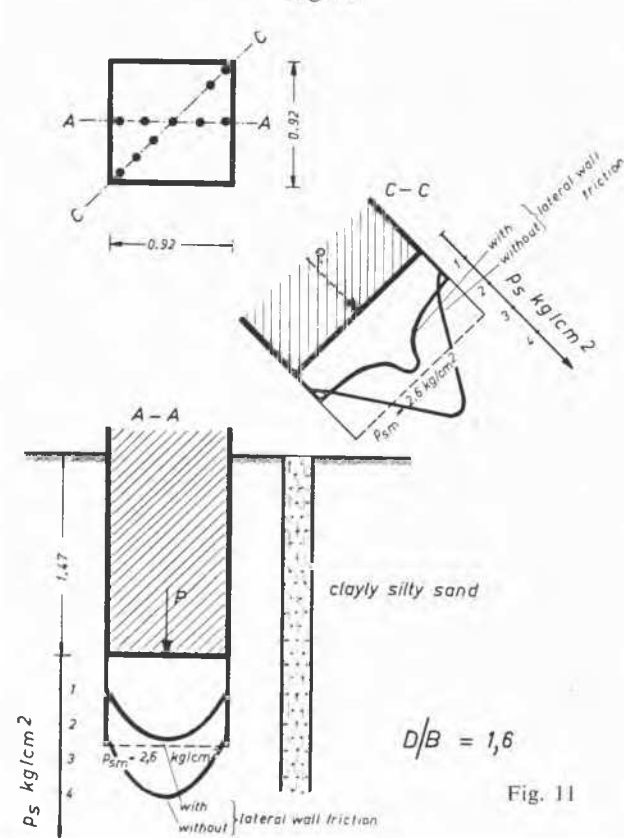


Fig. 11

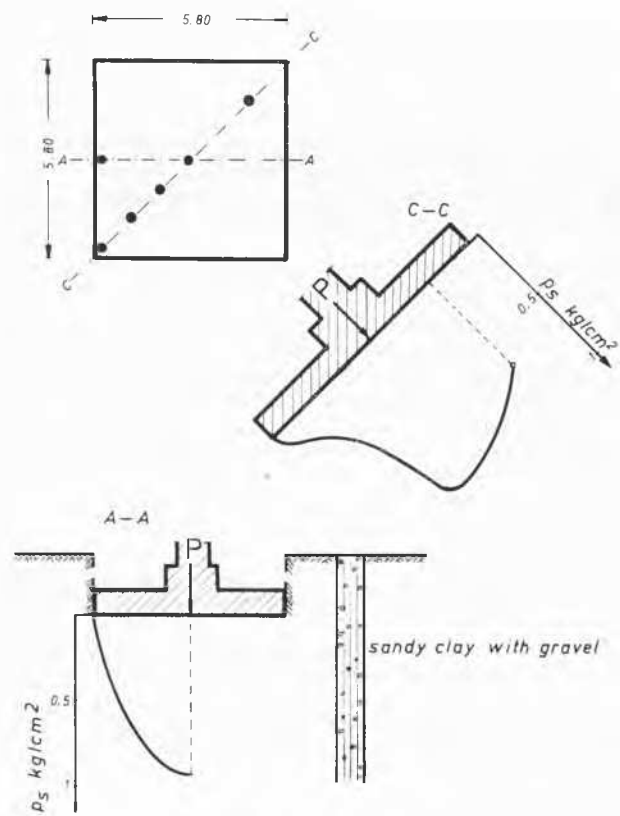


Fig. 12

Caissons are particularly suitable for the installation of pressure gauges.

Measurements beneath the foundations of buildings must be accepted with great caution, because the installation of pressure gauges is generally very difficult. In drawing graphs of results, the authors has rejected several measurements.

**2.1. Mainly concave parabolic distribution**—Out of eleven case records eight show an accumulation of pressure at the edges (Figs. 3-10). Most of these foundations rest on sand at a great depth, but results are also available of a structure on boulder clay (Fig. 8) where a concave parabola was also measured. The concrete block having a diameter of 11·3 m was set up solely for the purpose of test loading and was provided with adequate measuring instruments. In order to eliminate lateral friction, the structure was surrounded by a well, which removed the lateral earth pressure. The measured distribution of pressure agrees closely with that indicated by theory.

**2.2. Full parabolic distribution**—There are, however, other observations made on finished structures which show

a full parabolic distribution of pressure. They all apply to clay soils (Figs. 11-13).

The author considers that these are the only published cases in which pressure distribution is fully parabolic. Moreover, these cases depend on earlier measurements made at a time when very little experience of pressure gauges was available. Thus, with the exception of (Fig. 8) there is a dearth of reliable observations on cohesive soils. In view of the divergence in the measurements with Berlin boulder clay (Fig. 8) it would be premature if, without further aid, we were to seek an explanation for these variations. It is possible however that with soft clays must assume a predominantly plastic flow even with allowance for a generous factor of safety. That would mean that the ground creeps beneath the structure, which is generally the case with clay. On the other hand, with very firm boulder clay a much brittle failure is likely to occur.

Therefore, one reaches the conclusion that the assumption on which the determination of the contact pressure distribution in the elastic-plastic state is based, is in close agreement with practical experience.

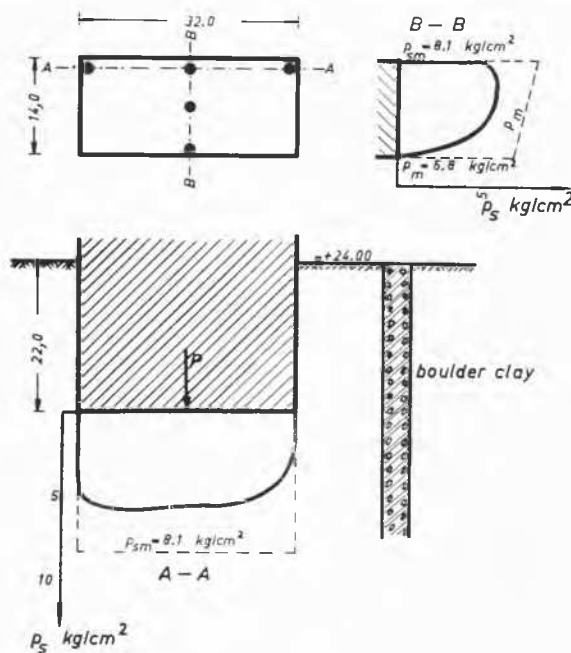


Fig. 13 Contact pressure distribution measured under the west-caisson of Niederfinow ship-lift (1934).  $D/B = 1\cdot 6$ .

Distribution des pressions mesurées sous le caisson Ouest du monte-charge pour bateaux Niederfinow (1934).  $D/B = 1\cdot 6$ .

After : DETIG (1934). Die Zwischenpfeiler der Kanalbrücke des Schiffshebewerkes Niederfinow. Baut. 12, p. 522.